ACS APPLIED MATERIALS & INTERFACES

Letter

www.acsami.org

Effect of Photogenerated Charge Transfer on the Photocatalysis in High-Performance Hybrid Pt−Co:ZnO Nanostructure Photocatalyst

Yongchun Lu, Yanhong Lin,* Tengfeng Xie, Liping Chen, Shasha Yi, and Dejun Wang*

College of Chemistry, Jilin University, Changchun, 130012, P. R. China

Supporting Information

ABSTRACT: Hybrid Pt−Co:ZnO nanostructure photocatalysts were prepared via a facile two-step synthetic strategy. SPS and TPV investigations demonstrate the existence of the synergetic effect between Pt and Co dopants. Such synergetic effect could make use of visible photons as well as facilitates the separation of photogenerated charges to prevent recombination, effectively prolongating the charges lifetime to participate photocatalytic reaction. The synergetic effect exist in Pt−Co:ZnO inducing as high as 7.7-fold in photovoltaic response and 10-fold in the photo−activity for hybrids compared to Co:ZnO.

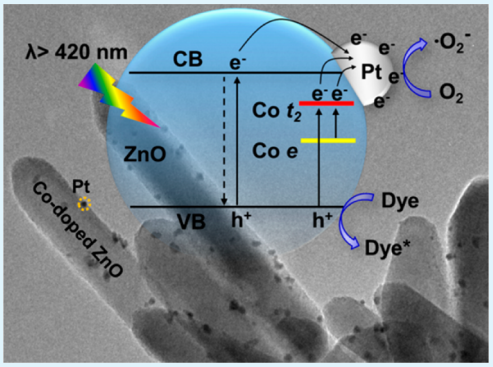

KEYWORDS: *hybrid nanostucture, Pt−Co:ZnO, synergetic effect, photovoltaic properties, photocatalytic activity*

INTRODUCTION

Efficient transfer and separation of photogenerated charges play a pivotal role in the process of solar energy conversion through photovoltaic or photocatalytic reactions. Semiconductors such as ZnO have been the subject of extensive investigation for last decades. In particular, the coupling of semiconductor nanocrystals with noble metal cocatalysts has proven to be effective in photocatalysis.[1−3] Noble metal cocatalysts, as a mediator to storage and discharge electrons through Fermi level equilibration between semiconductor and metal nanoparticles, which offers a higher quantum yield of photogenerated electrons transfer processes by promoting interfacial charge-transfer in these composite systems, are highly desirable for usage in a large number of photocatalytic reactions.[4−8] Among various noble-metal cocatalysts, Pt nanoparticles (NPs) has attracted considerable attention as one of the most promising candidates due to its larger work function (∼5.93 eV) related to semiconductors,[9] and thus Pt can provide a directly rapid photogenerated electron transfer channel from an excited semiconductor to the Pt NPs. Despite the enhancement of activity achieved by coupling semiconductor with Pt NPs, one disadvantage of Pt for photocatalysis applications is none Plasmon absorption in the visible and thus scarcely makes contribution to the visible photoresponse capacity of semiconductor.[10] In view of this issue, some new attempts have been made to combine noble metals with ion-doped semiconductor. Zhou and co-workers introduced a solar-energy transduction systems composed of Pt-loaded and N-doped TiO_2 for water splitting.[11] In this system, N-doped TiO_2 can capture visible photons and Pt-loaded TiO_2 promote charge separation. Thereby, it is highly desirable to design and fabricate novel catalysts with both rapid electron transfer and visible photoresponse capabilities.

Recently, we reported a preliminary study on Co-doped ZnO system in photocatalytic applications, which exhibits extremely high visible light-driven photooxidative capabilities for organic contaminants decomposition.[12] Here, we present a general strategy to synthesize Pt-loaded and Co-doped ZnO (Pt−Co:ZnO) hybrid catalysts into a one-dimensional nanostructure. The purposes of having such catalysts are listed as follows: (i) to improve charge separation and transfer, (ii) to extend the photoresponse into the visible-light region, and (iii) to understand mechanism and kinetic details of photogenerated charges separation and transfer processes in photocatalytic reactions by means of surface photovoltage spectra (SPS) and transient photovoltage (TPV) techniques. Although most of the photocatalytic studies focus on the net photoconversion efficiency, investigations on the understanding of charges separation and transfer at the surface or interface at the fundamental level is still lacking. Therefore, this work presents a new approach to enhance the photocatalytic performance and utilization of ZnO-based photocatalyst.

RESULTS AND DISCUSSION

The precursor Co:ZnO nanorods were first fabricated through an alcoholics process, serving as the starting templates for the subsequent load of Pt NPs (experimental details in the Supporting Information). The morphologies of pre−prepared

Received: February 27, 2013
Accepted: April 29, 2013
Published: April 29, 2013

   dx.doi.org/10.1021/am4007484 | ACS Appl. Mater. Interfaces 2013, 5, 4017−4020

pure ZnO and precursor Co:ZnO are exhibited in Figure S1. TEM technique was used to further characterize the samples. As displayed in Figure 1, a uniform distribution of dark spots on

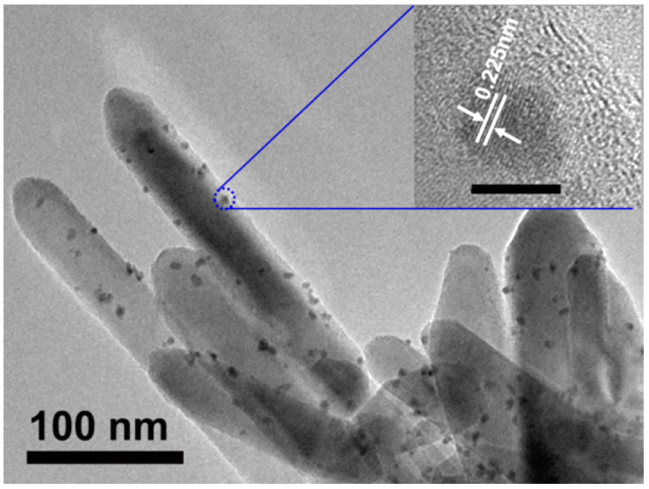

Figure 1. TEM image of Co:ZnO nanorods containing 1.47 mol % Pt NPs: Pt were homogeneously dispersed on the nanorods. Inset: HRTEM image of the selected area, in which Pt deposited on the nanorods are clearly evident, scale bar: 5 nm.

the nanorods are found with very small particle size of ~5 nm, and the HRTEM image confirms that the dark spots are Pt NPs with the lattice spacing of 0.225 nm originating from the (111) plane of metallic Pt (JCPDS no. 04−0802).

Typical XRD patterns of the pre−prepared samples are shown in Figure S2 in the Supporting Information. Clearly, all peaks in the XRD profile can be indexed to the hexagonal wurtzite structure of ZnO (JCPDS no. 36−1451). However, no obvious diffraction peaks of metallic Pt are observed. The chemical state of Pt in Pt−Co:ZnO hybrids were further analyzed by XPS. As presented in Figure S3a in the Supporting Information, the emergence of two fitted peaks of Pt $4f_{5/2}$ at 70.35 eV and Pt $4f_{7/2}$ 73.71 eV can be assigned to Pt^0.[13] The presence of Pt^0 further indicates that the Pt species are in the metallic state. In addition, the XPS spectrum of the Co 2p (see Figure S3b in the Supporting Information) clearly shows the presence of Co species in hybrid system even though there is a somewhat high noise. The contents of Pt and Co species in the surface layer are listed in Table S1 in the Supporting Information, respectivly. Figure S4 in the Supporting Information is the UV−vis DRS of the samples. As displayed, compared with pure ZnO, precursor Co:ZnO sample shows two features: one is the red shift of absorbance band−edge (400−520), which can be attributed to a strong electronic interaction between the Co species and ZnO. The other one is the additional absorbance band appearing in the visible light region (520−700) induced by the d→d internal transitions of Co^{2+} ions.[14] As expected, in contrast to pure ZnO and precursor Co:ZnO, the prominent feature of Pt−Co:ZnO is that the overall visible-light absorbance intensities are enhanced. The overall light-harvesting enhancements could be attributed to the hybrids system derived from the synergetic effect between Pt and Co dopant. Particularly, Co dopant can make use of visible photons as well as be Pt-loaded to the outer surface of Co:ZnO, facilitating charge separation and transfer, which will improve their photocatalytic performance.

Hybrid photocatalytic performances are explored for the degradation of alizarin red (AR) dyes under UV and visible-light irradiation (λ > 420 nm and λ > 510 nm), respectively. The kinetics of AR degradation followe a pseudo first order reaction at low dye concentrations: $\ln(c_0/c) = kt$, where k is the apparent rate constant.[15] First, Pt−Co:ZnO show superior catalytic activity to pure ZnO as well as precursor Co:ZnO in the presence of UV light (Figure 2a). Second, compared with

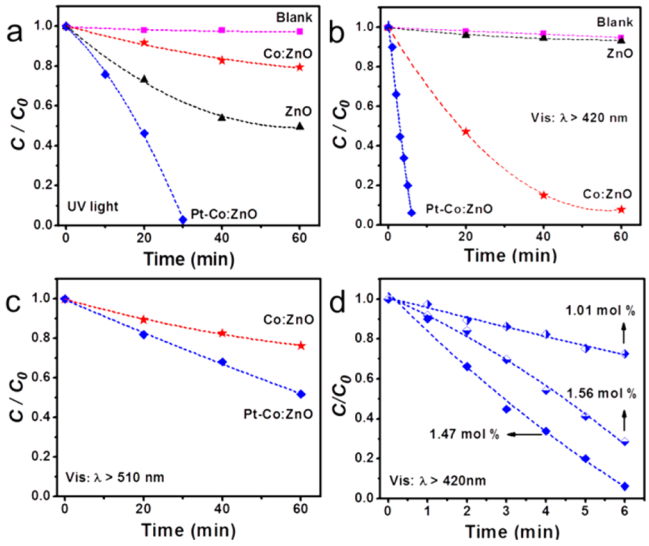

Figure 2. Kinetics of photodegradation of AR in the presence of as−prepared samples using different irradiation wavelengths (a) UV light, (b) visible light with λ > 420 nm, and (c) visible light with λ > 510 nm, respectively. (d) Photodegradation of AR by Pt−Co:ZnO hybrids with a varying amount of Pt added under visible light (λ > 420 nm) irradiation.

pure ZnO and Co:ZnO, Pt−Co:ZnO can effectively harvest visible light and exhibit higher photocatalytic activity under visible light (λ > 420 nm) irradiation. As reflected in Figure 2b, pristine ZnO exhibited negligible catalytic activity, whereas Pt−Co:ZnO (k = 0.474 min^{-1}) displayed approximately ten times higher rate of dye degradation than that of Co:ZnO (k = 0.0433 min^{-1}). Third, it can be seen from Figure 2c that the catalytic activity of Pt−Co:ZnO (k = 0.011 min^{-1}) sample is ca. two times as high as Co:ZnO (k = 0.005 min^{-1}) with λ > 510 nm visible-light irradiation. It is well-known that the photocatalytic activity is mainly governed by phase structure, adsorption ability, and separation efficiency of photogenerated electron−hole pairs. On the basis of the discussion above, the crystal phase structure does not evidently change and cannot be regarded as the major factor that accounts for the significant enhancement of the photocatalytic activity of ZnO. Therefore, the high photocatalytic activity of Pt−Co:ZnO is supposed to be the consequence of the enhanced light adsorption as well as the efficient charge separation and transportation induced by the synergetic effects between Pt and Co dopant. In addition, it was interesting to find that the performance of the Pt−Co:ZnO with 1.47 mol % Pt catalyst is far superior to that with the 1.01 mol % and 1.56 mol % catalysts, and the former one only 6 min to decompose ~95% of AR in aqueous solution (Figure 2d), indicating that there is an optimal modification concentration of Pt NPs in Pt−Co:ZnO hybrids. The corresponding absorption spectrum of an aqueous solution of AR in the presence of the 1.47 mol % Pt in hybrids evolutions with visible

light (λ > 420 nm) time is presented in Figure S5 in the Supporting Information.

The SPS technique is an effective tool for the investigation of the photogenerated charges separation and transfer properties in photocatalyst system and may provide useful information for understanding the catalytic mechanism of the material. We display the SPS with in-phase signals (indexed with x) which are direct proof of charge separation and the directionality of charge transfer.[16] As mirrored in Figure 3, for pure ZnO (A_x), a

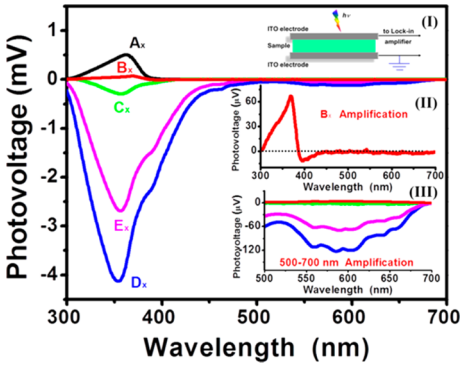

Figure 3. SPS of the Pt−Co:ZnO hybrid with different amounts of Pt added (B) 0 mol %, (C) 1.01 mol %, (D) 1.47 mol %, and (E) 1.56 mol %, compared with (A) pure ZnO. SPS signals shown in phase with excitation (solid lines: A_x, B_x, C_x, D_x, and E_x). Inset: (I) schematic setup of SPS measurement; (II) the enlarged SPS of 0 mol % Pt−Co:ZnO sample; (III) the enlarged SPS curves in the region 520−700 nm.

positive response peak located at ∼360 nm is observed, implying that the positive charges (holes) move toward the surface of sample. As for precursor Co:ZnO (B_x), there are two interesting changes in contrast to the SPS of pure ZnO: on the one hand, a relative weak positive response is observed in UV−light region, which may be due to an increase in surface defects that act as the electron−hole recombination centers with the incorporation of Co doping in ZnO; on the other hand, unlike the SPS response in the UV-light region, where an extended negative response in visible-light region are observed (see Figure 3 inset II), which should be attributed to the charge transfer transition between the Co dopant and ZnO. However, hybrid samples loaded with Pt show broader and stronger negative photovoltage response band in the whole region.

According to the SPS results, the Pt−Co:ZnO hybrids show two prominent features: one is that all the hybrids exhibit negative photovoltage signals. The other one is that the maximum values for photovoltage response intension increase (the highest increase up to about 7.7 times (D_x)) with the loaded Pt NPs. Regarding the photocatalytic activities tests, we divide the SPS signals into three response bands to illustrate the photogenerated charge transfer properties of hybrids. For the UV response band in the range 300−400 nm, the modification of Pt on the surface of Co:ZnO will repair the defects induced by the doping of Co,[17] and act as electron acceptor to achieve the photogenerated electrons transfer from Co:ZnO to Pt. Therefore, Pt load promotes charge separation and transfer as well as effectively inhibits the recombination of photogenerated charge carriers, which results in a remarkable photovoltage response in UV−light region. The SPS response threshold values red shift to the range 400−520 nm, which is thought to be the band gap narrow due to the formation of localized state dopant energy levels of Co in the band gap of ZnO.[18] Therefore, under visible-light irradiation, the photogenerated electrons (e^-) can easily transfer from the valence band (VB) of ZnO to the dopant energy level, i.e., the charge transfer transition between the Co and ZnO in hybrid. Furthermore, the modification of Pt provides a secondary transfer path for the separate photogenerated charge[19] under the action of charge transfer transition, and thus greatly improves the charge separation efficiency and reduces its recombination rate, leading to a superior photoresponse capacity. As for the response in the range 520−700 nm, as reported in the literature,[14] the response around this region is probably due to the d→d internal transitions of Co dopant. Nevertheless, d→d transition is a localized state transition and plays an unimportant role on the contribution to the visible SPS signals (see Figure 3 inset III). However, the work function of the metal determines the electron transfer direction, since the working function of Pt is 5.93 eV, whereas that of ZnO is 5.2 eV,[20] once the two materials are placed in contact, Pt will provide an ohmic contact, a difference of 0.73 eV would result in electron transfer from ZnO to Pt until the Fermi levels equilibrate. Such a type of contact is supposed to render quick discharge of a certain amount of electrons at the localized state dopant energy levels. Thus, after the modification of Pt on the surface of Co:ZnO an obvious visible SPS signal presents. In summary, the synergetic effect of Pt and Co dopant in our Pt−Co:ZnO hybrids plays a significant role in the transition of photogenerated charges, potentially offering desirable effciency for separating and tranfering photogenerated charges. Furthermore, the transfer behavior of photogenerated charges has a distinct effect on the photoactivity, resulting in the observed increase in photocatalytic activity under both UV and visible light. In addtion, as shown in Figure 3 inset III, whereas the Pt-modified quantity further improves from 1.47 mol % (D_x) to 1.56 mol % (E_x), the excess Pt NPs will cover the surface and hinder the light absorption of hybrid, reducing the photogenerated charges separation rate. Consequently, for the 1.56 mol % Pt-modified sample, the UV and visible SPS responses exhibit an unexpected decrease. These anlysis are consistent with all our experimental results of photocatalytic activities (Figure 2).

TPV measurements are used to further investigate the impact of the synergetic effects on the transfer properties of photogenerated charges of Pt−Co:ZnO hybrid nanostructures. As reflected in Figure 4, the samples are excited with a 532 nm laser, when the intensity of the laser pulse (excitation level) is

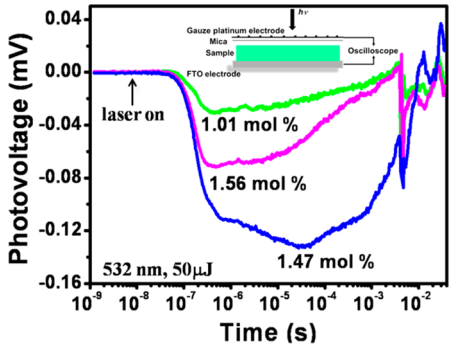

Figure 4. TPV spectra of the Pt−Co:ZnO hybrid with different amount of Pt added. The wavelength of the laser are 532 nm with a laser radiation pulse with a power of 50 μJ. Inset: schematic setup of TPV measurement.

dx.doi.org/10.1021/am4007484 | ACS Appl. Mater. Interfaces 2013, 5, 4017−4020

50 μJ, and TPV signals of the Pt−Co:ZnO hybrids are displayed on a logarithmic time scale. According to the TPV results, the following features are obtained: (1) all the hybrids exhibit negative TPV signals, which indicate that photogenerated electrons transfer from Co:ZnO into Pt NPs after excitation by the laser pulse; (2) the 1.47 mol % Pt-modified sample presents the maximum values for TPV responses, indicating that most photogenerated charge carriers separate in hybrids; (3) there is an obvious decay for TPV peak of the 1.47 mol % Pt-modified sample on the millisecond time scale. The delay for TPV peak means the time retardation needed for the whole the separation and recombination process, which is supposed to include the photogenerated charge transfer from the VB of ZnO to the Co dopant energy level, and then migrate into Pt NPs. This charge transfer process may be beneficial to reduce the recombination of photogenerated electron−hole pairs and prolongs the lifetime of photogenerated charges, which is most pronounced for the 1.47 mol % Pt-modified sample. In our experiments, the SPS and TPV characterizations are closely connected with the performance of photocatalyst. According to the above analysis of SPS and TPV data, the possible photogenerated charge transfer processes in the Pt−Co:ZnO hybrids photocatalysts are summarized in Scheme S1 in the Supporting Information. Undoubtedly, these results will be of benefit in the design of catalysts with high sunlight-driven photocatalytic activity.

CONCLUSIONS

In conclusion, the Pt−Co:ZnO hybrid nanostructure photocatalysts have been successfully prepared by a simple two−step wet−chemistry approach. The hybrids show a wide absorption region in the solar spectrum. SPS and TPV investigations demonstrate the existence of the synergetic effects of Pt and Co dopant in our Pt−Co:ZnO hybrids. Noticeably, the synergetic effect plays a significant role in the behaviors of photogenerated charges, potentially offers desirable effciency for separating and tranfer photogenerated charges. Furthermore, the transfer behavior of photogenerated charges has a distinct relationship to the photoactivity, resulting in the superior photocatalytic activity under both UV and visible light.

ASSOCIATED CONTENT

Supporting Information

Experimental details, XRD patterns, XPS spectra, UV−vis DRS, UV−vis absorption spectra of photodegradation of AR using 1.47 mol % Pt modified Co:ZnO nanorods under visible light illumination (λ > 420 nm), the possible mechanism of photogenerated charge transfer in the Pt−Co:ZnO hybrid system. This material is available free of charge via the Internet at http://pubs.acs.org/.

AUTHOR INFORMATION

Corresponding Author

*E-mail: linyh@jlu.edu.cn (Y.L.); wangdj@jlu.edu.cn (D.W.). Tel/Fax: +86-431-85168093.

Notes

The authors declare no competing financial interest.

ACKNOWLEDGMENTS

This work is supported by National Basic Research Program of China (973 Program, 2013CB632403), National Natural Science Foundation of China (21173103 and 51172090), Science and Technology Developing Funding of Jilin Province (201115012), and Program for Graduate Innovation Fund of Jilin University (20121046).

REFERENCES

(1) Henglein, A. *Chem. Rev.* **1989**, *89*, 1861−1873.
(2) Kamat, P. V. *J. Phys. Chem. B* **2002**, *106*, 7729−7744.
(3) Kudo, A.; Miseki, Y. *Chem. Soc. Rev.* **2009**, *38*, 253−278.
(4) Lin, D. D.; Wu, H.; Zhang, R.; Pan, W. *Chem. Mater.* **2009**, *21*, 3479−3484.
(5) Harris, C.; Kamat, P. V. *ACS Nano* **2010**, *4*, 7321−7330.
(6) Li, P.; Wei, Z.; Wu, T.; Peng, Q.; Li, Y. D. *J. Am. Chem. Soc.* **2011**, *133*, 5660−5663.
(7) Ye, M. D.; Gong, J. J.; Lai, Y. K.; Lin, C. J.; Lin, Z. Q. *J. Am. Chem. Soc.* **2012**, *134*, 15720−15723.
(8) Ma, Y.; Qian, X.; Zong, X.; Wang, D.; Wu, G. P.; Wang, X.; Li, C. *Energy Environ. Sci.* **2012**, *4*, 6345−6351.
(9) Lin, J. M.; Lin, H. Y.; Cheng, C. L.; Chen, Y. F. *Nanotechnology* **2006**, *14*, 4391−4394.
(10) Subramanian, V.; Wolf, E.; Kamat, P. V. *J. Phys. Chem. B* **2001**, *105*, 11439−11446.
(11) Zhou, H.; Li, X. F.; Fan, T. X.; Osterloh, F. E.; Ding, J.; Sabio, E. M.; Zhang, D.; Guo, Q. X. *Adv. Mater.* **2009**, *21*, 1−6.
(12) Lu, Y. C.; Lin, Y. H.; Wang, D. J.; Wang, L. L.; Xie, T. F.; Jiang, T. F. *Nano Res.* **2011**, *4*, 1144−1152.
(13) Morikawa, T.; Ohwaki, T.; Suzuki, K. I.; Moribe, S.; Tero-Kubota, S. *Appl. Catal., B* **2008**, *83*, 56−62.
(14) Kim, Y. D.; Cooper, S. L.; Klein, M. V.; Jonker, B. T. *Phys. Rev. B: Condens. Matter Mater. Phys.* **1994**, *49*, 1732−1742.
(15) Wang, X. H.; Li, J. G.; Kamiyama, H.; Moriyoshi, Y.; Ishigaki, T. *J. Phys. Chem. B* **2006**, *110*, 6804−6809.
(16) Gross, D.; Mora-Seró, I.; Dittrich, T.; Belaidi, A.; Mauser, C.; Houtepen, A. J.; Da Como, E.; Roqach, A. L.; Feldmann, J. *J. Am. Chem. Soc.* **2010**, *132*, 5981−5983.
(17) Norberg, N. S.; Gamelin, D. R. *J. Phys. Chem. B* **2005**, *109*, 20810−20816.
(18) Wang, B. Q.; Xia, C. H.; Iqbal, J.; Tang, N. J.; Sun, Z. R.; Lv, Y.; Wu, L. *Solid State Sci.* **2009**, *11*, 1419−1422.
(19) Kamat, P. V. *J. Phys. Chem. Lett.* **2012**, *3*, 663−672.
(20) Özgür, Ü.; Alivov, Y. I.; Liu, C.; Teke, A.; Reshchikov, M. A.; Doğan, S.; Avrutin, V.; Cho, S. -J.; Morkoc, H. *J. Appl. Phys.* **2005**, *98*, 041301.